Journal of Organometallic Chemistry 693 (2008) 2572–2578

Contents lists available at ScienceDirect

Journal of Organometallic Chemistry

journal homepage: www.elsevier.com/locate/jorganchem

Synthesis, crystal structure and thermal behavior of dimethylgold(III) derivatives of salicylaldimine Schiff bases – Novel precursors for gold MOCVD applications

Aleksandr A. Bessonov [a,b,*], Natalia B. Morozova [a], Nikolay V. Gelfond [a], Pyotr P. Semyannikov [a], Iraida A. Baidina [a], Sergey V. Trubin [a], Yuriy V. Shevtsov [a], Igor K. Igumenov [a]

[a] Nikolaev Institute of Inorganic Chemistry of Siberian, Branch of Russian Academy of Sciences, Lavrentiev Avenue 3, Novosibirsk 630090, Russia
[b] Novosibirsk State University, Novosibirsk, Russia

ARTICLE INFO

Article history:
Received 15 February 2008
Received in revised form 8 April 2008
Accepted 22 April 2008
Available online 30 April 2008

Keywords:
Organogold(III) precursors
X-ray structure
Vapour pressure
Thermal decomposition
Gold MOCVD
Gold nanoparticles

ABSTRACT

Dimethylgold(III) complexes with salicylaldimine Schiff bases of general formula $Me_2Au(Sal{=}N{-}R)$ (R = methyl (**1**), *iso*-propyl (**2**), or cyclohexyl (**3**)) have been synthesized in a single step reaction from dimethylgold(III) iodide $[Me_2AuI]_2$ and N-substituted salicylaldimines. Single-crystal X-ray studies provide evidence of mononuclear four-coordinated complexes with square-planar coordination geometry. The temperature dependences of saturated vapour pressure of complexes have been studied by the Knudsen effusion method with mass spectrometric analysis of the composition of the gas phase. The thermodynamic parameters of the sublimation process ΔH_T^o and ΔS_T^o have been calculated. Thermal decomposition of the vapour of compounds has been studied by means of high temperature mass spectrometry in a vacuum, and by-products have been determined. All of these complexes show good volatility and thermal stability. For complex **2**, which is more volatile and low-melting, pulse MOCVD experiments have been carried out at substrate temperatures lower than 200 °C. The deposited gold nanoparticles (5–15 nm) have been investigated by means of SEM and AFM.

1. Introduction

Gold nanomaterials have important applications in optical devices [1–3], solar cells [4], and for nano and microelectronics [5–8]. Other applications include use gold nanoparticles as catalytic systems for epoxidation of propylene, and CO oxidation at low temperature when deposited with high dispersion on the surface of TiO_2, Fe_2O_3, and Al_2O_3 [9–12]. Moreover, catalytic activity of Au catalysts strongly depends on formation conditions and particle size [13–15]. Among various deposition methods under consideration, metal organic chemical vapour deposition (MOCVD) attracts more attention because it allows us to obtain gold coatings as ultra-fine particles [9], thin films [16,17], and gold crystals [18,19]. Chemical vapour deposition of volatile organometallic compounds is widely used for formation of metallic and oxide coatings on different substrates. Depositions on surfaces of solids with highly developed porous structures are being considered as a valuable method for the preparation of catalysts with high dispersion of active components [10]. Besides that, the MOCVD method allows effective control of the size of the forming gold particles [10]. However, the study of gold MOCVD processes has been somewhat limited by the lack of suitable precursors [7]. The most popular precursors for the MOCVD of gold coatings are dimethylgold(III) β-diketonates [20–22]. On a base of our experience, these complexes are air, moisture and light sensitive, and suffer from poor stability during storage [23,24]. That's why the search for and investigation into alternative precursors of gold MOCVD is an important problem. Earlier, we investigated dimethylgold(III) carboxylates as precursors for the production of gold films. Volatility and thermal properties of these compounds were studied [25,26]. Salicylaldimine class of ligands have been chosen in reported studies because of there are some advantages in stabilization of dimethylgold(III) using mixed oxygen nitrogen ligand sphere (N,O-coordination) [27]. The use of more stable volatile precursors will allow to improve gold MOCVD procedure. Moreover, the studies of thermal behavior of gold compounds in solid state and gas phase, mechanisms of interaction of precursor vapour with hot surface can be very useful at choosing of MOCVD parameters. The deposition temperature might be found on the basis of thermal decomposition of precursor vapour, the evaporator temperature – from measurements of vapour pressure of precursor. Investigations of thermal properties and volatility of precursors play an important role in gold MOCVD development.

This paper reports the synthesis, structure and thermal properties of dimethylgold(III) derivatives of salicylaldimine Schiff bases $Me_2Au(Sal{=}N{-}R)$, where R = Me (**1**), Pr^i (**2**), or Cy (**3**). Compounds

* Corresponding author. Address: Nikolaev Institute of Inorganic Chemistry of Siberian Branch of Russian Academy of Sciences, Lavrentiev Avenue 3, Novosibirsk 630090, Russia. Tel.: +7 383 3309556; fax: +7 383 3309489.
E-mail address: bessonov@che.nsk.su (A.A. Bessonov).

0022-328X/$ - see front matter © 2008 Elsevier B.V. All rights reserved.
doi:10.1016/j.jorganchem.2008.04.028

have been characterized by elemental analysis, mass spectrometry, X-ray, IR, and ^{1}H NMR spectroscopy. Complexes **1** and **3** were described earlier [28], but there were not details in structure and thermal behavior. Dimethylgold(III) salicylaldimine chelates are air and moisture stable and don't require special conditions for storage. The compounds are soluble in most common organic solvents, have low-melting points and evaporate almost quantitatively at low temperatures in a vacuum. Our investigations report that dimethylgold(III) complexes with N-substituted salicylaldimines are viable precursors for MOCVD of gold materials.

2. Experimental

2.1. General information and materials

Dimethylgold(III) iodide $[Me_2AuI]_2$ was prepared from $KAuCl_4$ ($\geqslant$98%) using the method [29]. Salicylaldimines HSal=N–R (R = methyl, *iso*-propyl, or cyclohexyl) were synthesized from salicylaldehyde (Fluka, purum, $\geqslant$98%) and alkylamines (Merck, puriss., $\geqslant$99%) by the literature procedure [30]. All reactions were carried out using Schlenk techniques.

Elemental analyses were performed on a Carlo Erba 1106 instrument. IR spectra were recorded in KBr on a FT-IR Scimitar FTS 2000. ^{1}H NMR spectra were recorded on an MSL Bruker 300 spectrometer; with $CDCl_3$ as solvent. Melting points were determined by Kofler m.p. apparatus.

The saturated vapour pressure of complexes **1**–**3** was measured by the Knudsen effusion procedure combined with mass spectrometric analysis of the gas phase composition. Detailed descriptions of the measurement method, calibration procedure and experimental technique are presented in [31]. The temperature ranges were 58–87 °C for **1**, 48–78 °C for **2**, and 65–111 °C for **3**. The thermodynamic parameters of the sublimation process ΔH^o_T and ΔS^o_T have been calculated from the temperature dependencies of saturated vapour pressure.

Mass spectra were obtained on a MI-1201 spectrometer; the energy of ionizing electrons was 35 eV. The vapour temperature of the complexes was 70 °C (**1**), 60 °C (**2**), and 90 °C (**3**).

The thermal decomposition process of the vapour of compounds **1** and **2** on a heated surface was studied by means of high temperature mass spectrometry. The precursors were transferred to the gas phase at a temperature of 100 °C for **1**, and 80 °C for **2**. Detailed descriptions of the method and set-up can be found in [27].

Scanning electron microscopy (SEM) was carried out using a JSM-6700F. The morphology of gold nanoparticles samples deposited by pulse MOCVD technique was examined by a Solver Pro (NT-MDT) atomic force microscope (AFM).

2.2. Synthesis of complexes

$[Me_2AuI]_2$ and $NaHCO_3$ were added to a methanol solution of the equimolar amount of HSal=N–R. The mixture was stirred in argon flow at room temperature for 7 h. The methanol was removed in vacuo and the residue was redissolved in hexane. The hexanes solution was filtered and the volatile components were removed in vacuo. The substance was purified by recrystallization from hexane at −10 °C and the pale yellow crystals were formed.

The yield of complex **1** was 84%, m.p. 101–103 °C (lit. data 103 °C [28]). Spectral data for **1**: IR (ν, cm^{-1}) (C–H)(Au–CH_3) 2977 m, 2915 m; (C=N) 1633 vs; (C–O) 1188 m, 1152 m, 1124 m. ^{1}H NMR δ 1.02 (s, 3H, Au–CH_3), δ 1.23 (s, 3H, Au–CH_3), δ 3.63 (s, 3H, N–CH_3), δ 6.56–7.40 (4H, ArH), δ 8.19 (s, 1H, N=C–H). Anal. Calc. for $C_{10}H_{14}AuNO$: C, 33.2; H, 3.9; N, 3.9. Found: C, 33.4; H, 4.0; N, 3.8%.

The yield of complex **2** was 90%, m.p. 78–79 °C. Dimethylgold(III) *N-iso*-propyl-salicylaldiminate (**2**) has been prepared for the first time. Spectral data for **2**: IR (ν, cm^{-1}) (C–H)(Au–CH_3) 2977 m, 2907 m; (C=N) 1624 vs; (C–O) 1174 m, 1150 m, 1127 m. ^{1}H NMR δ 0.94 (s, 3H, Au–CH_3), δ 1.22 (s, 3H, Au–CH_3), δ 1.35 (d, 6H, CH_3), δ 4.35 (m, 1H, N–CH), δ 6.55–7.40 (4H, ArH), δ 8.24 (s, 1H, N=C–H). Anal. Calc. for $C_{12}H_{18}AuNO$: C, 37.0; H, 4.7; N, 3.6. Found: C, 37.2; H, 4.6; N, 3.6%.

The yield of complex **3** was 85%, m. p. 111–112 °C (lit. data 114 °C [28]). Spectral data for **3**: IR (ν, cm^{-1}) (C–H)(Au–CH_3) 2921 s, 2853 m; (C=N) 1618 vs; (C–O) 1189 m, 1143 m, 1128 w. ^{1}H NMR δ 0.92 (s, 3H, Au–CH_3), δ 1.21 (s, 3H, Au–CH_3), δ 1.35–2.04 (10H, CH_2), δ 3.82 (m, 1H, N–CH), δ 6.53–7.40 (4H, ArH), δ 8.20 (s, 1H, N=C–H). Anal. Calc. for $C_{15}H_{22}AuNO$: C, 42.0; H, 5.2; N, 3.3. Found: C, 42.1; H, 5.2; N, 3.4%.

2.3. X-ray crystallography

X-ray powder pattern diffraction data were collected on a DRON-3M diffractometer using Cu Kα-radiation in 2θ angles range of 5–50° at 296 K. X-ray diffraction data reveal a monophase system for complexes **1**–**3**. Single-crystal X-ray studies were performed on a Bruker-Nonius X8Apex (Mo Kα-radiation) instrument [32]. Crystals of **1**–**3** (pale yellow needles) were grown from the hexanes solution at −10 °C. The structure was determined using the SHELXTL program and refined using full-matrix least-squares. All non-hydrogen atoms were refined anisotropically, whereas hydrogen atoms were placed at the calculated positions and included in the final stage of refinements with fixed parameters. Crystallographic refinement parameters of complexes **1**–**3** are summarized in Table 1. The atomic coordinates and selective bond distances and angles of these complexes are presented in (Tables 4 and 5 Supplementary material).

2.4. Pulse MOCVD experiments

A horizontal hot wall pulse MOCVD system was used for depositions on silicon substrates. The apparatus for depositions is drawn schematically in Fig. 1. MOCVD depositions of gold nanoparticles were performed under O_2 flow from the precursor **2**. Silicon (100) discs 0.5 mm thick and 40 mm in diameter were used as substrates. The substrate temperature was controlled in the 190–200 °C range. The base pressure of the reactor was maintained below 10^{-2} Torr.

Deposition of gold particles was carried out in the following cycle manner: (1) The reactor was vacuumed to residue pressure of 10^{-2} Torr. (2) The vacuum valve was closed, then the valve on the line, connecting the vapourizer with the reactor, was opened and a portion of precursor vapour was injected into the system under the force of saturated vapour pressure. The time of injection was 5 s. (3) The oxygen valve was opened until the pressure in the reactor became ~7 Torr. (4) After introduction of oxygen, the system was kept up for 15 s. Then the vacuum valve was opened and a new deposition cycle was started.

For deposition of gold nanoparticles, 20 cycles were carried out.

3. Results and discussion

3.1. Synthesis

In paper [28], compounds **1** and **3** were earlier synthesized from thallium salts of salicylaldimines and $[Me_2AuI]_2$ with 62% and 52% yields accordingly. We offered a modified procedure with *N*-alkylsalicylaldimine as ligand source. The synthetic method, including reaction of $[Me_2AuI]_2$ with the corresponding HSal=N–R, gives

Table 1
Crystal data and structure refinement parameters for complexes **1**, **2** and **3**

	1	**2**	**3**
Empirical formula	$C_{10}H_{14}AuNO$	$C_{12}H_{18}AuNO$	$C_{15}H_{22}AuNO$
Formula weight	361.19	389.25	429.30
Temperature (K)	150(2)	100(2)	150(2)
Crystal system	Rhombic	Triclinic	Monoclinic
Space group	*Aba*2	$P\bar{1}$	$P2_1/c$
A (Å)	16.016(3)	7.142(1)	11.8472(4)
B (Å)	18.656(4)	8.896(2)	8.9313(2)
C (Å)	6.961(1)	10.259(2)	14.2890(5)
α (°)	90	109.36(3)	90
β (°)	90	93.69(3)	106.788(1)
γ (°)	90	96.32(3)	90
Volume (Å^3)	2080.0(7)	607.7(2)	1447.49(8)
Z	8	2	4
D_{Calc} (g/cm^3)	2.307	2.122	1.970
Absorption coefficient (mm^{-1})	14.106	12.079	10.152
F(000)	1344	366	824
Crystal size (mm)	0.70 × 0.22 × 0.18	0.26 × 0.08 × 0.05	0.05 × 0.30 × 0.04
Crystal color	Pale yellow	Pale yellow	Pale yellow
Θ Range (°)	3.35–32.60	2.12–28.33	2.72–27.47
Index ranges	$-24 \leqslant h \leqslant 20$, $-28 \leqslant k \leqslant 27$, $-10 \leqslant l \leqslant 6$	$-9 \leqslant h \leqslant 9$, $-11 \leqslant k \leqslant 11$, $-13 \leqslant l \leqslant 13$	$-15 \leqslant h \leqslant 14$, $-7 \leqslant k \leqslant 11$, $-17 \leqslant l \leqslant 18$
Reflections collected	10574	5264	10756
Independent reflections [R_{int}]	3162 [0.0268]	4540 [0.0180]	3318 [0.0218]
Data/restraints/parameters	3162/1/131	4540/143/290	3318/0/229
Goodness-of-fit on F^2	1.044	1.106	1.030
Final *R* indices [$I > 2\sigma(I)$]	$R_1 = 0.0164$	$R_1 = 0.0496$	$R_1 = 0.0192$
	$wR_2 = 0.0366$	$wR_2 = 0.1365$	$wR_2 = 0.0448$
R indices (all data)	$R_1 = 0.0194$	$R_1 = 0.0541$	$R_1 = 0.0233$
	$wR_2 = 0.0372$	$wR_2 = 0.1400$	$wR_2 = 0.0459$
Largest difference in peak and hole (e/Å^3)	1.273 and −1.611	8.645 and −2.344	1.666 and −0.765

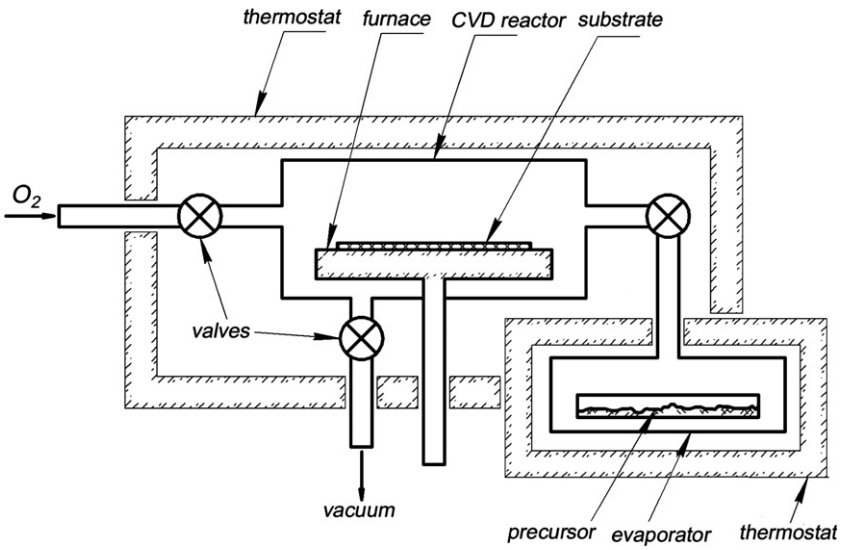

Fig. 1. Scheme of pulse MOCVD apparatus.

the products $Me_2Au(Sal{=}N{-}R)$. This method allows removal of the stage of production of thallium derivatives of salicylaldimines. With our method, yields of products were 84–90%. It should be noted that compound **2** was synthesized and characterized for the first time.

3.2. X-ray single crystal structure

The compounds' structures are molecular, formed from neutral molecules $(CH_3)_2Au(Sal{=}N{-}R)$. The crystal structure of relative compound, dimethylgold(III) *N*-phenylsalicylaldiminate (R = phenyl), was published earlier [33]. Structures of complexes **1**, **2** and **3** are shown in Figs. 2–4, correspondingly. Gold atoms in molecules have a slightly distorted square-planar configuration formed by oxygen and nitrogen atoms of salicylaldimine ligand and two carbon atoms of methyl groups. The average Au–O bond in **1** (2.082 Å) is longer than similar bonds found in **2** (2.075 Å) and **3** (2.071 Å), while the average Au–N distances (2.118 Å) are slightly smaller than in **2** (2.125 Å) and **3** (2.124 Å) (Table 2). Au–CH_3 bond length is typical for dimethylgold(III) derivatives – 2.039 and 2.031 Å for **1** and **3** accordingly [34] although in one of the independent complexes, **2**, this value is larger (2.070 Å) (Table 2). Angle °AuN in complexes **1** and **2** has the same value (91.2°), while in **3** this angle is 90.6°. Molecules of **1** are planar with accuracy of ±0.027 Å (with the exception of hydrogen atoms of methyl groups). Crystal molecules are packed in infinite stacks along the *Z* axis with Au···Au

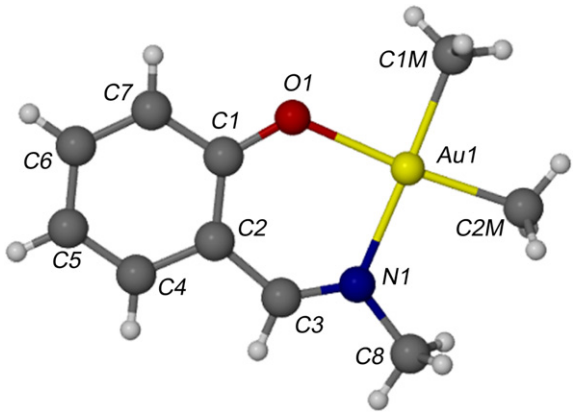

Fig. 2. Plot of complex **1** showing the atom numbering scheme for the core atoms.

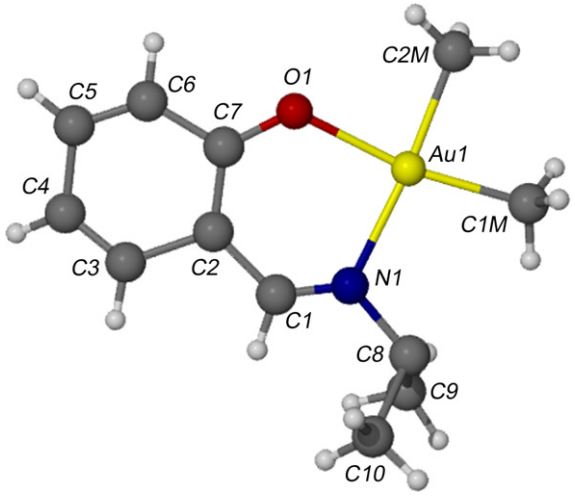

Fig. 3. Plot of complex **2** showing the atom numbering scheme for the core atoms.

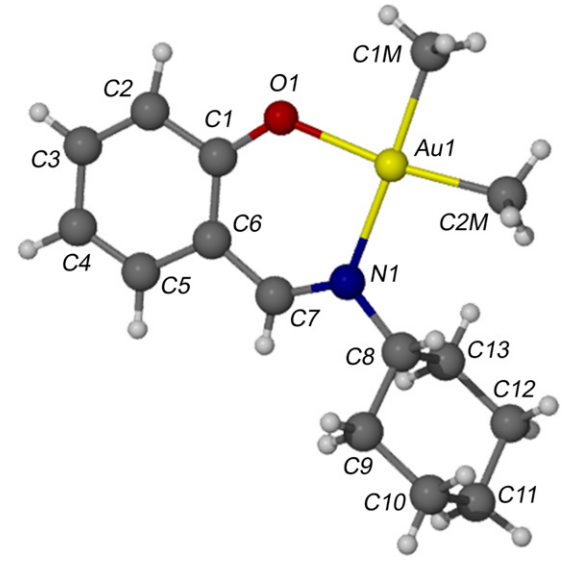

Fig. 4. Plot of complex **3** showing the atom numbering scheme for the core atoms.

distance of 3.492 Å and AuAuAu angle of 170.6°. The angle between normal to the plane of molecule **1** and stack axis is 12.2°. Molecules **2** are planar with accuracy of 0.084 Å, with the exception of isopropyl hydrogens. Au···Au distance between neighbour molecules in stack is 3.835 Å. Molecules of complex **3**, with the exception of atoms of cyclohexyl ring, are also planar with accuracy of ±0.014 Å. Au···Au distance between neighbour molecules is 4.660 Å. Increasing of Au···Au distance in the unit cell of **3** in comparison with **1** and **2** is going on due to insertion of more large substituents in the ligand (Table 2).

Distances between centres of stacks in **1** are >7.75 Å, the shortest intermolecular distances H···H in the crystal are about 2.40 Å. In complex **2**, intermolecular interactions °···H type in stacks are estimated as 2.53–3.37 Å. The structure of **3** has a lamellar character; molecules are packed in layers (1 0 0) with distances of 11.34 Å to each other. °···H distances between molecules **3** are equal to 2.52 and 3.53 Å.

So, by X-ray data it is shown that changing of the alkyl substituent at the nitrogen atom in dimethylgold(III) salicylaldimine chelates provides minimal influence on the geometry of coordination centre and closest bond distances. Although the character of packing of molecules in crystal varies, it has an influence on the thermal properties of complexes. Insertion of larger substituents decreases the compound density (Table 2) and increases distances between gold atoms of neighbour molecules in stacks. In Table 2, some comparative crystallographic parameters and geometric characteristics of complexes **1**–**3** are shown.

3.3. Mass spectra

Analysis of mass spectra has shown that vapour of compounds **1**–**3** consists of molecular forms. The main ions in mass spectrum of **1** – $[Me_2AuSal{=}N{-}Me]^+$ (I_{rel} = 43%) and $[AuSal{=}N{-}Me]^+$ (I_{rel} = 100%); **2** – $[Me_2AuSal{=}N{-}Pr^i]^+$ (I_{rel} = 52%) and $[AuSal{=}N{-}Pr^i]^+$ (I_{rel} = 100%); **3** – $[Me_2AuSal{=}N{-}Cy]^+$ (I_{rel} = 34%), $[AuSal{=}N{-}Cy]^+$ (I_{rel} = 100%), and $[Sal{=}N{-}Cy]^+$ (I_{rel} = 15%). The same data were observed for salicylaldimine class of ligands earlier [28]. The process of fragmentation of molecular ions is similar for all compounds. The molecular ion becomes a fragment after elimination of methyl groups and the ligand.

In the investigated temperature ranges (58–87 °C for **1**, 48–78 °C for **2**, and 65–111 °C for **3**), the relative intensity of the ion peaks in the mass spectra of complexes **1**–**3** remains unchanged. This evidences that the vapours of complexes are thermally stable in these temperature ranges.

3.4. Volatility studies

The Knudsen effusion procedure with mass spectrometric analysis of the composition of gas phase was used to measure the temperature dependencies of the saturated vapour pressure (*P*–*T* dependencies) of complexes **1**–**3** (Fig. 5). Based on the *P*–*T* dependencies, the thermodynamic parameters of the sublimation process were calculated (Table 3). Temperature dependences of vapour pressure are presented in Fig. 5, and thermodynamic data as the equation $\lg(P, \text{Torr}) = A - B/(T, \text{K})$, ΔH°_{T} and ΔS°_{T} are shown in Table 3. Statistical processing of the experiments was based on the vapour pressure measured at several values of temperature. The *P*–*T* curves show that compound **2** is the most volatile in the investigated temperature range. Substitution of the methyl group in **1** by cyclohexyl in the salicylaldimine ligand (compound **3**) causes a decrease of the volatility within the studied temperature range (Fig. 5). Complex **3** has considerably lower volatility than **1** and **2**. Such a difference is likely to be connected with the effects of crystal packing of the complexes. The volatility row of investigated dimethylgold(III) complexes with salicylaldimine Schiff bases is (for $P = 10^{-3}$ Torr): **2** (61 °C) > **1** (70 °C) > **3**(96 °C) (Table 3, Fig. 5).

We compared vapour pressure of complexes **1**–**3** and other dimethylgold(III) precursors used for gold MOCVD (Fig. 5):

Table 2
Compared X-ray characteristics of complexes **1**, **2** and **3**

Complex	V/Z (Å^3)	ρ_{meas} (g/cm^3)	d (Å)				
			Au–O	Au–N	Au–C(Me)	Au···Au in layer	N–C(R)
1	260.0	2.307	2.082	2.118	2.039	3.492	1.469
2	303.8	2.122	2.075	2.125	2.050	3.835; 4.570	1.490
3	361.9	1.970	2.071	2.124	2.031	4.660	1.487

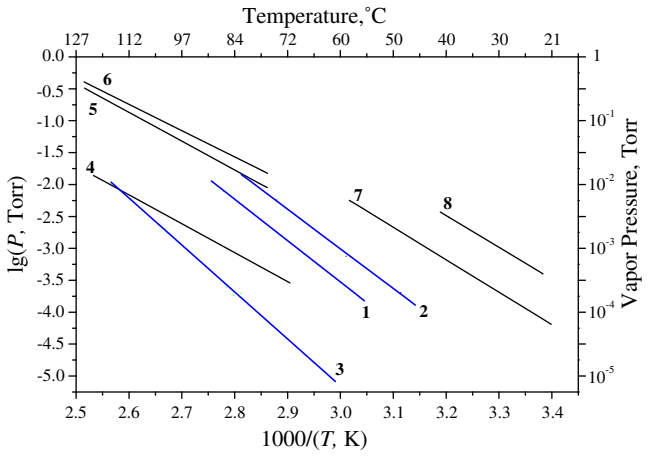

Fig. 5. Temperature dependencies of saturated vapour pressure for (1) – Me_2Au-(Sal=N–Me), (2) – Me_2Au(Sal=N–Pr^i), (3) – Me_2Au(Sal=N–Cy), (4) – Me_2Au(ba) [10], (5) – Me_2Au(tta) [35], (6) – Me_2Au(bfa) [36], (7) – Me_2Au(kaa) [10], and (8) – Me_2Au(acac) [10].

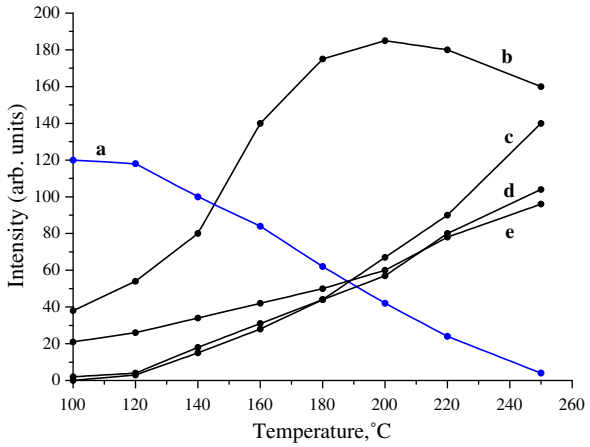

Fig. 6. Temperature dependence of intensities of ion peaks at decomposition of **1** vapour; main ions: (a) – $[AuSal{=}N{-}Me]^+$ (331 m/z), (b) – $[CH_2Sal{=}N{-}Me]^+$ (148 m/z), (c) – $[HSal{=}N{-}Me]^+$ (135 m/z), (d) – $[C_2H_5Sal{=}N{-}Me]^+$ (163 m/z), (e) – $[Sal{=}N{-}Me]^+$ (134 m/z).

Me_2Au(ba) (**4**) – dimethylgold(III) 1-phenyl-1,3-butanedionate (Knudsen method) [10], Me_2Au(tta) (**5**) – dimethylgold(III) 1,1,1-trifluoro-4-(2-thienyl)-1,3-butanedionate (flow method) [35], Me_2Au(bfa) (**6**) – dimethylgold(III) 1,1,1-trifluoro-4-phenyl-1,3-butanedionate (flow method) [36], Me_2Au(kaa) (**7**) – dimethylgold(III) 2-imino-4-pentaneonate (Knudsen method) [10], and Me_2Au(acac) (**8**) – dimethylgold(III) 2,4-pentanedionate (Knudsen method) [10]. Complexes **1** and **2** reveal volatility similar to **5** and **6** (Fig. 5). Precursors **7** and **8** are more volatile compounds than **1** and **2** in the studied temperature ranges. Complex **3** has vapour pressure close to **4** (Fig. 5). Thus, dimethylgold(III) salicylaldimine chelates show sufficient volatility for their applications as MOCVD precursors.

3.5. Thermal decomposition

Thermolysis of vapour of complexes **1** and **2** on hot surface as more volatile and perspective MOCVD precursors was studied in a vacuum by high temperature mass spectrometry (Figs. 6 and 7). From the analysis of temperature dependences of relative intensities of main ion peaks in mass spectra of thermolysis products, the temperatures of beginning of decomposition of complexes in gas phase were determined. In our experimental conditions,

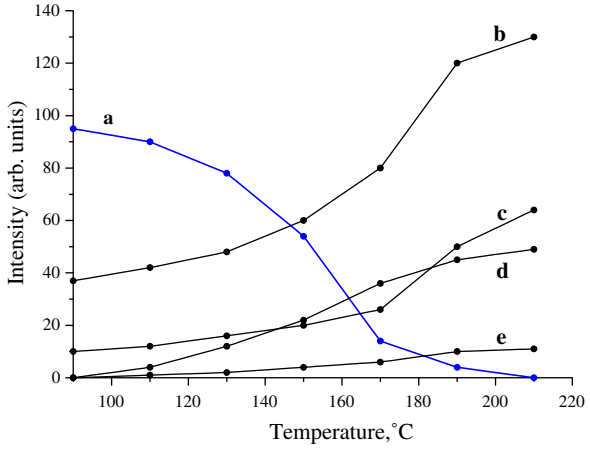

Fig. 7. Temperature dependence of intensities of ion peaks at decomposition of **2** vapour; main ions: (a) – $[AuSal{=}N{-}Pr^i]^+$ (359 m/z), (b) – $[Sal{=}N{-}C_2H_5]^+$ (148 m/z), (c) – $[HSal{=}N{-}Pr^i]^+$ (163 m/z), (d) – $[CH_2Sal{=}N{-}Pr^i]^+$ (177 m/z), and (e) – $[C_2H_5$-$Sal{=}N{-}Pr^i]^+$ (191 m/z).

thermodecomposition of molecules in gas state on heated surface is started at a temperature higher than 120 ± 5 °C for **1** and 110 ± 5 °C for **2** (Figs. 6 and 7). Exchange of methyl group of salicyl-

Table 3
Thermodynamics parameters of sublimation processes of complexes **1–3**

Complex	m.p. (°C)	Number of points	lg(P, Torr) = $A - B/(T, K)$		Temperature range (°C)	ΔH_T^o (kJ mol^{-1})	ΔS_T^o (J mol^{-1} K^{-1})
			A	$B \times 10^{-3}$			
1	101–103	4	15.9 ± 0.1	6.48 ± 0.04	58–87	123.9 ± 0.8	250.0 ± 1.9
2	78–79	5	15.6 ± 0.4	6.21 ± 0.14	48–78	118.8 ± 2.7	243.2 ± 7.6
3	111–112	9	16.9 ± 0.3	7.35 ± 0.12	65–111	140.6 ± 2.2	268.1 ± 5.7

aldimine ligand in **1** to *iso*-propyl results in decreasing of the temperature of beginning of decomposition of complex **2** vapour. The main volatile organic products of thermolysis of complex **1** are HSal=N–Me, MeSal=N–Me, and EtSal=N–Me. Thermodecomposition products of vapour of compound **2** have similar composition: HSal=N–Pr^i, MeSal=N–Pr^i, and EtSal=N–Pr^i. The data obtained provide arguments about the same scheme of thermodecomposition of vapour of complexes **1** and **2** on hot surface. It was suggested as:

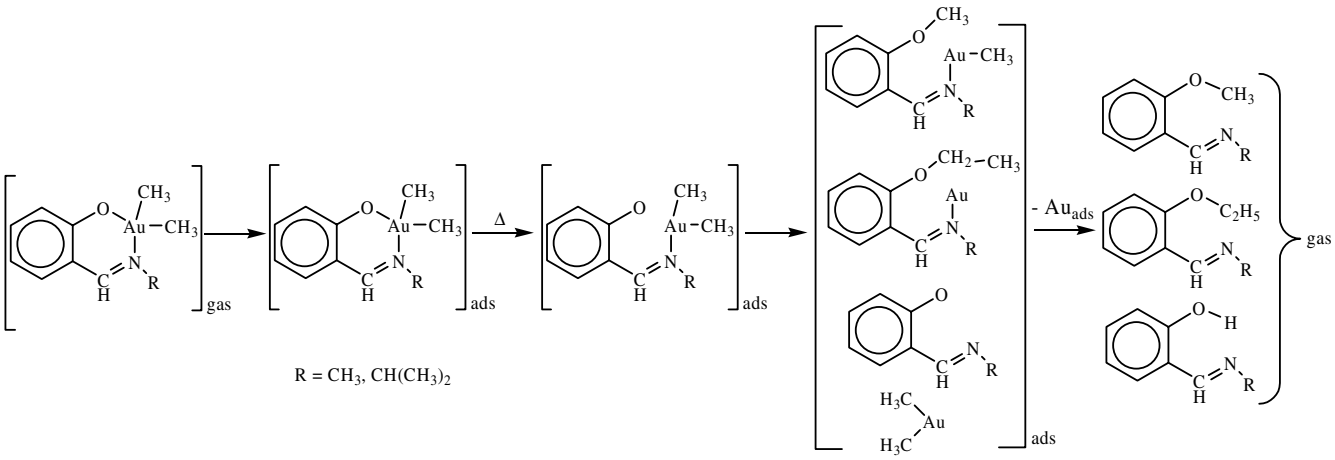

Among the main products of thermolysis of complexes, there are salicylaldimine Schiff bases and their derivatives. This indicates the consecutive cleavage of methyl groups and ligand with the formation of metal gold. The methyl groups migrate from gold to ligand in adsorbed state on surface. For other dimethylgold(III) derivatives it was observed a formation of ethane at thermodecomposition of vapour [25,27]. Besides that, in solution $Me_2Au(acac)$ also decomposes with loss of ligand and methyl groups, which is indicated by the presence of ethane and acetylacetone among the main products of decomposition [37]. In case salicylaldimine derivatives C_2H_6 was not found among volatile organic products of thermolysis.

Change of the relative intensity of gold-containing ion peak $[AuSal{=}N{-}Me]^+$ for **1** (Fig. 6a) and $[AuSal{=}N{-}Pr^i]^+$ for **2** (Fig. 7a) allows us to trace the decomposition rate of precursor vapours. In such experimental conditions, complex **1** demonstrates a lower rate of thermolysis than **2** (Figs. 6 and 7). Gold-containing fragments are absent among the decomposition products of complex **2** even at 210 ± 5 °C: in the case of precursor **1** this is only at 260 ± 5 °C (Figs. 6 and 7). So, thermodecomposition of vapour phase of complex **2** occurs more quickly. Introduction of oxygen into the reactor does not lead to substantial change of the decomposition mechanism and kinetics of the process. Oxidation of the decomposition product was observed, and results in the absence of carbon in thermolysis products.

3.6. Pulse MOCVD depositions

The MOCVD experiments were conducted on a horizontal hot wall reactor using complex **2** as the gold source reagent and oxygen as a co-precursor. As was shown in the investigation of thermodecomposition, oxygen as co-precursor does not affect the mechanism of decomposition of the precursor on the surface of substrate, but allows decreasing of the carbon content as impurities. We selected complex **2** as the precursor simply because of its higher volatility and lower melting point. Parameters of MOCVD experiments were selected on the basis of analysis of volatility data and thermal properties of the precursor. The temperature of Si substrate in the range 190–200 °C was selected on the basis of thermodecomposition data of complex **2** vapour (in this range there is absence of gold-containing ions in mass spectra, Fig. 7). The size of deposited gold particles alters in the range of 5–15 nm, as was measured by the SEM and AFM technique (Figs. 8 and 9). As shown in Figs. 8 and 9, gold nanoparticles were deposited with even distribution on the surface of silicon substrate. A further increase in the temperature to 210 °C results in further increase of particle concentration on the surface. Particle size is also about 10 nm.

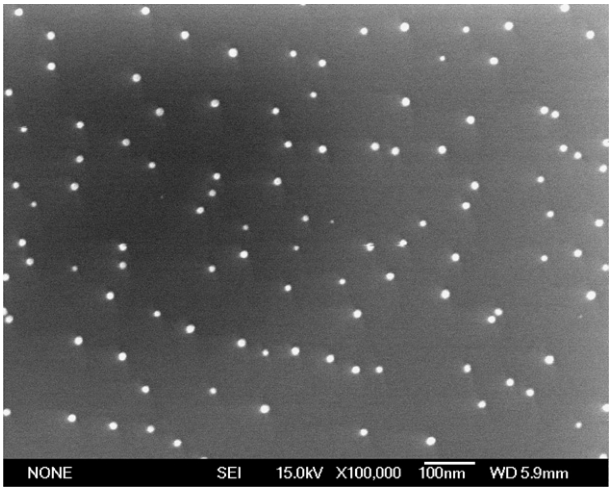

Fig. 8. SEM of gold nanoparticles deposited on Si substrate at 190–200 °C.

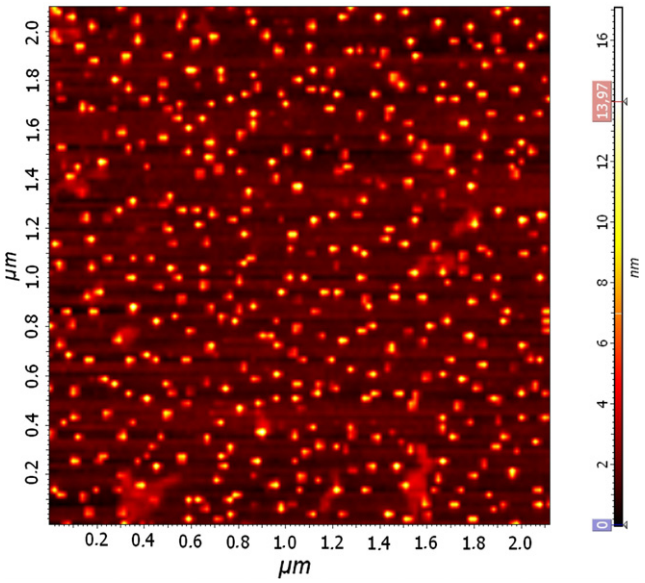

Fig. 9. AFM of gold nanoparticles deposited on Si substrate at 190–200 °C.

4. Conclusions

This study shows that dimethylgold(III) complexes with salicylaldimine Schiff bases are viable MOCVD precursors to gold materials. These compounds are stable during storage and have a good volatility. On the basis of X-ray data, it is shown than exchange of substituent at donor nitrogen atom in ligand have great impact on the character of packing and so on resulting in differences of thermal properties. Thus, complex **2** has the highest volatility among the presented compounds, while the introduction of cyclohexyl in molecules dramatically decreases the volatility. Besides, vapour of complex with *iso*-propyl group has lesser thermal stability in comparison with *N*-methylsubstituted salicylaldiminate although mechanism and by-products of thermolysis are similar. So, introduction of various substituents in ligand of dimethylgold(III) complex allows modifying of thermal properties and volatility of compounds in a wide range.

Dimethylgold(III) derivatives of salicylaldimine Schiff bases can be used in gold MOCVD at deposition temperatures lower than 200 °C with better mass transport properties and thermal behavior than used gold β-diketonates derivatives. Although optimization of the deposition conditions and investigation of obtained gold materials will be necessary in the future, the thermal behavior and volatility characteristics of precursors make them attractive candidates for gold MOCVD processes.

Acknowledgements

The authors thank the Russian Science Support Foundation for financial support. Anton I. Smolentsev provided technical assistance with the crystal structure determinations. SEM and AFM analyses were carried out by Dr. V.S. Danilovich and N.G. Semerikov.

Appendix A. Supplementary material

CCDC 678139, 678140 and 678141 contain the supplementary crystallographic data for **1**, **2** and **3**. These data can be obtained free of charge from The Cambridge Crystallographic Data Centre via www.ccdc.cam.ac.uk/data_request/cif. Supplementary data associated with this article can be found, in the online version, at doi:10.1016/j.jorganchem.2008.04.028.

References

[1] J. Kashammer, P. Wohlfart, J. Weiß, C. Winter, R. Fischer, S. Mittler-Neher, Opt. Mater. 9 (1998) 406–410.
[2] L. Armelao, D. Barreca, G. Bottaro, A. Gasparotto, S. Gross, C. Maragno, E. Tondello, Coord. Chem. Rev. 250 (2006) 1294–1314.
[3] I.C.S. Carvalho, F.P. Mezzapesa, P.G. Kazansky, O. Deparis, M. Kawazu, K. Sakaguchi, Mater. Sci. Eng. C 27 (2007) 1313–1316.
[4] Y.-F. Lu, M. Takai, S. Nagamoto, K. Kato, S. Namba, Appl. Phys. A 54 (1992) 51–56.
[5] M. Jubber, J.I.B. Wilson, J.L. Davidson, P.A. Fernie, P. John, Appl. Surf. Sci. 43 (1989) 74–80.
[6] T.H. Baum, P.B. Comita, Thin Solid Films 218 (1992) 80–94.
[7] T.T. Kodas, M.J. Hampden-Smith, The Chemistry of Metal CVD, VCH, Weinheim, New York, Basel, Cambridge, Tokyo, 1994.
[8] C. Schoßler, A. Kaya, J. Kretz, M. Weber, H.W.P. Koops, Microelectron Eng 30 (1996) 471–474.
[9] M. Okumura, K. Tanaka, A. Ueda, M. Haruta, Solid State Ion. 95 (1997) 143–149.
[10] P.P. Semyannikov, B.L. Moroz, S.V. Trubin, G.I. Zharkova, P.A. Pyryaev, M.Yu. Smirnov, V.I. Bukhtiyarov, J. Struct. Chem. 47 (2006) 458–464.
[11] M. Haruta, Catal. Today 36 (1997) 153–166.
[12] G.J. Hutchings, Catal. Today 72 (2002) 11–17.
[13] M. Valden, X. Lai, D.W. Goodman, Science 281 (1998) 1647–1650.
[14] M. Haruta, M. Date, Appl. Catal. A: Gen. 222 (2001) 427–437.
[15] M.S. Chen, D.W. Goodman, Science 306 (2004) 252–255.
[16] U. Hiroto, S. Noriyasu, S. Masamitsu, T. Masatuki, O. Katsumi, JP 06-101046, Mitsubishi Materials Corp., 1994, Appl. No. 04-274966.
[17] H. Masataka, EP 0571713A2, Fujitsu Limited 1993, Appl. N 931023808.
[18] T.H. Baum, C.R. Jones, J. Vac. Sci. Technol. B 4 (1986) 1187–1191.
[19] T.T. Kodas, T.H. Baum, P.B. Comita, J. Cryst. Growth 87 (1988) 378–382.
[20] T.H. Baum, C.R. Jones, Appl. Phys. Lett. 47 (1985) 538–540.
[21] C.E. Larson, T.H. Baum, R.L.J. Jackson, Electrochem. Soc. 134 (1987) 266.
[22] E. Feurer, H. Suhr, Appl. Phys. A44 (1987) 171–175.
[23] G.I. Zharkova, I.K. Igumenov, S.V. Zemskov, Koord. Khim. 6 (1980) 720–723.
[24] G.I. Zharkova, G.I. Tyukalevskaya, I.K. Igumenov, S.V. Zemskov, Koord. Khim. 14 (1988) 1362–1367.
[25] A.A. Bessonov, I.A. Baidina, N.B. Morozova, P.P. Semyannikov, S.V. Trubin, N.V. Gelfond, I.K. Igumenov, J. Struct. Chem. 48 (2007) 282–288.
[26] A.A. Bessonov, N.B. Morozova, N.V. Gelfond, P.P. Semyannikov, S.V. Trubin, Yu.V. Shevtsov, Yu.V. Shubin, I.K. Igumenov, Surf. Coat. Technol. 201 (2007) 9099–9103.
[27] P.P. Semyannikov, V.M. Grankin, I.K. Igumenov, G.I. Zharkova, J. Phys. IV 5 (1995) 213–220.
[28] K.S. Murray, B.E. Reichert, B.O. West, J. Organomet. Chem. 61 (1973) 451–456.
[29] A.A. Bessonov, N.B. Morozova, N.V. Kuratieva, I.A. Baidina, N.V. Gelfond, I.K. Igumenov, Russ. J. Coord. Chem. 34 (2008) 70–77.
[30] M. Dennstedt, J. Zimmermann, Chem. Ber. 21 (1888) 1553–1554.
[31] P.P. Semyannikov, I.K. Igumenov, S.V. Trubin, T.P. Chusova, Z.I. Semenova, Thermochim. Acta 432 (2005) 91–98.
[32] Bruker AXS Inc., APEX2 (Version 1.08), SAINT (Version 7.03), SADABS (Version 2.11) and SHELXTL (Version 6.12), Bruker Advanced X-ray Solutions, Madison, Wisconsin, USA, 2004.
[33] A.A. Bessonov, A.I. Smolentsev, I.A. Baidina, N.B. Morozova, Acta Crystallogr. E63 (2007) m3154.
[34] S. Shibata, K. Lijima, T.H. Baum, J. Chem. Soc., Dalton Trans. (1990) 1519–1520.
[35] U. Hiroto, S. Noriyasu, S. Masamitsu, O. Katsumi, JP 05-320170. Mitsubishi Materials Corp., 1993, Appl. No. 04-274929.
[36] U. Hiroto, S. Noriyasu, S. Masamitsu, T. Masayuki, O. Katsumi, JP 05-331176. Mitsubishi Materials Corp. 1993, Appl. 1 04-274967.
[37] R.B. Klassen, T.H. Baum, Organometallics 8 (1989) 2477–2482.